colloids and interfaces

MDPI

Article

Optical Switches for Lipid Membranes: Computed Molecular Projection Area as a Switch Selection Criterion

Ivan Boldyrev

Shemyakin–Ovchinnikov Institute of Bioorganic Chemistry, Russian Academy of Sciences, ul. Miklukho-Maklaya 16/10, 117593 Moscow, Russia; ivan@lipids.ibch.ru; Tel.: +7-495-330-66-10

Abstract: Optical switches in lipid membranes are an emerging tool to tune the properties of the bilayer or membrane protein integrated therein. Here, we use simple geometry and physics considerations to deduce structural criteria to design efficient photoactivated switches for lipid membranes. We compare how the area of projection on the bilayer of various classes of photoswitches changes upon the *trans/cis* or open/closed transition and show that azobenzene and stilbene should distort the bilayer structure the most. We also conclude that planar-elongated molecules, in which atoms of isomerizable double bond have no additional substituents, while substituents of the fragments adjacent to the double bond prevent formation of the planar molecule in *cis* configuration, are to be the best photoswitches for lipid membranes.

Keywords: optical switches; molecular motors; *trans–cis* isomerism; lipid bilayer; lipid membrane; lateral stress profile

Citation: Boldyrev, I. Optical Switches for Lipid Membranes: Computed Molecular Projection Area as a Switch Selection Criterion. *Colloids Interfaces* **2022**, *6*, 30. https://doi.org/10.3390/colloids6020030

Academic Editor: Wuge Briscoe

Received: 30 March 2022
Accepted: 5 May 2022
Published: 9 May 2022

1. Introduction

Molecular motors are molecules that transform external energy into mechanical energy. The best-known molecular motor is the myosin protein. It transforms chemical energy stored in ATP into muscle contraction. The efficiency of laboratory-tailored molecular motors is many times lower than that of myosin; therefore, such molecules have not gained application yet. However, the ongoing work in this direction is intensive.

Optical switches are a type of molecular motors; they change conformation under the effect of light. To produce a controlled effect on a lipid bilayer, special optical switches are being developed. These switches are promising membrane permeability regulators or antimicrobial agents inducing membrane lysis. The optical switch activity is regulated by an external stimulus, i.e., the light of a specific wavelength.

Lipid chemistry utilizes azo-dyes as optical switches. Azo-dyes structurally similar to fatty acids and lipids have been synthesized back in 1980s, but the first report on the application of isomerization of an azo-dye to control natural lipid membrane properties was published by Fujiwara and Yonezawa in 1991 [1]. Later on, Song, Perlstein, and Whitten developed phospholipids with azobenzene integrated in the acyl chains [2]. However, lipid and fatty acid-based optical switches drew intense attention by the end of 2000s and have been growing ever since. We consider as landmark works the recent publications on the application of optical switches to control lipid phase segregation behavior in membranes [3–5] or modulate protein kinase C [6], TRPV1 receptor activity [7], or model ion channels [8].

Practically, in all known cases, the optical switches based on unsubstituted azobenzene are used in lipid membrane. There has been a single report on ortho-fluoro derivatives of azobenzene applied [9]. However, optical switches as such are represented by a rather wide range of structures, which, in addition to azobenzene derivatives, include derivatives of alkene, green fluorescent protein chromophore, structures based on retinal and hemithioindigo dye, diarylethene, spirooxazine, spiropyran, and donor-acceptor Stenhouse adducts (DASA). The aim of this work is to elucidate the applicability of these classes of molecules as optical switches in lipid membranes.

2. Objects and Methodology

2.1. Objects

Today, photoswitches are based on reactions of *E/Z* isomerization of azobenzenes, alkenes (such as stiff-stilbene and particularly sterically hindered alkenes), retinal analogs (NABP and NAIP), derivatives of green fluorescent protein (GFP), and hemithioindigo. For a detailed description, see the example review [10]. Another type of photoswithes is based on the ring open/close reaction of DASA [11], diarylethene [12,13], spiropyran [14,15], and spirooxazine [14]. Photoswitches possess diverse chemical structures. Figure 1 presents the molecules used in the work.

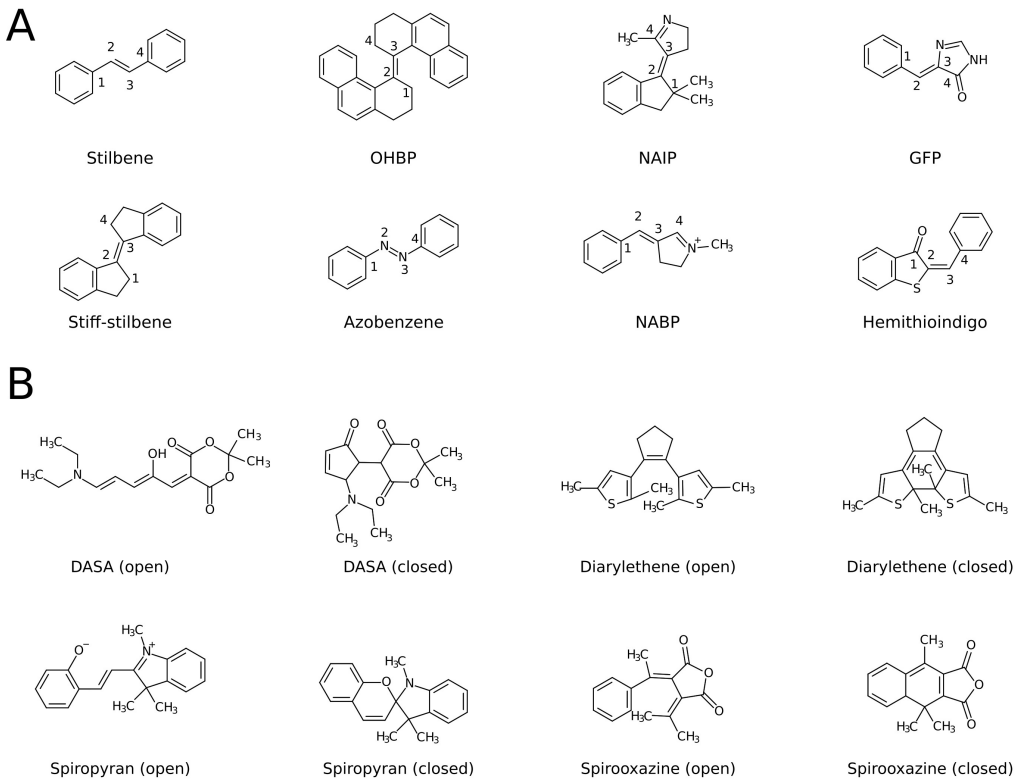

Figure 1. Structures of molecules used in the work. (**A**) Optical switches based on *cis*/*trans* isomerism (*E/Z*-switches). OHBP, trans1,1′,2,2′,3,3′,4,4′octahydro4,4′biphenanthrylidene (an overcrowded alkene); NAIP, Nalkylated indanylidene pyrroline (retinal analog); GFP, green fluorescent protein fluorophore; NABP, Nalkylated benzylidene pyrroline (retinal analog). (**B**) Optical switches based on ring open/closed reaction (*O/C*-switches). DASA, donor-acceptor Stenhause adducts. For the sake of simplicity merocyanine and fulgide are named as open forms of spyropyran and spyrooxazine, respectively.

E/Z photoswitches are molecules combining two fragments joined by a C=C or N=N double bond. The two fragments can be either in an *trans* or *cis* configuration with respect to the double bond. Change of the configuration occurs upon irradiation with a light of the appropriate wavelength.

Open/closed (*O/C* photoswitches are molecules able reversibly form intramolecular cycles upon irradiation with a light of the appropriate wavelength.

2.2. Physical Model

Two factors act upon a hydrophobic molecule in the lipid bilayer. The first factor is hydrophobicity. The alien molecule arranges in the bilayer so that the area of contact between its hydrophobic surface and water is minimal. The factor pushes the alien molecule deeper in the bilayer. Inside the bilayer, in the area of the lipid tails, the packing density is high, or in other words, the lateral pressure is high. The pressures are directed perpendicular to

the normal bilayer (that is parallel to the surface). The value of the lateral pressures varies along the depth of the bilayer. The variation is described by the lateral pressures profile. The latter can be obtained by molecular modeling (MD) [16] or analytically [17,18]. The profiles obtained by MD are lipid structure specific. However, the general shape of the profile is the same independently of the method.

The energy of a molecule inside a lipid bilayer can be equaled to the work spent on the expansion of the lipid monolayer against the lateral pressure

$$W = \int_{z_0-\frac{z_1}{2}}^{z_0+\frac{z_1}{2}} A(z)P(z)dz \quad (1)$$

where z is the coordinate on the axis parallel to the average lipid tail direction; z_0 is the coordinate of the center of the mass of the molecule in the bilayer; z_1 is the molecule length along the axis; $A(z)$ is the molecule cross-section area in the plane perpendicular to the lipid bilayer normal; and $P(z)$ is the lateral pressure applied to this area. (See Figure 2 for the explanation; also, the approach has been applied for fluorescent lipid probes [19] and lipophilic prodrugs [20]).

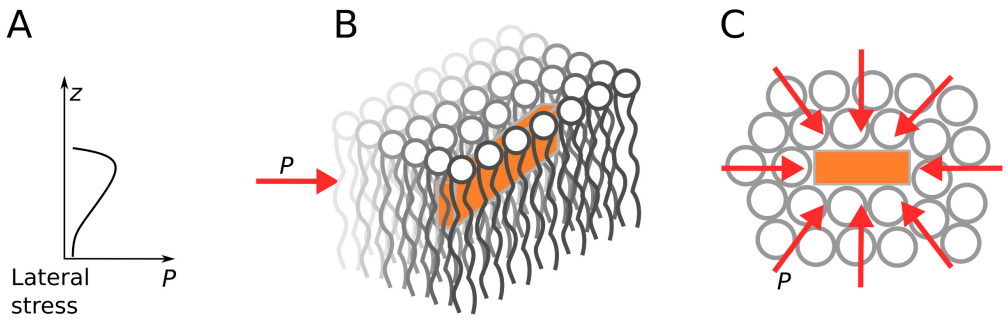

Figure 2. (**A**) Lateral pressure profile in the hydrophobic region. (**B**) Schematic representation of a molecule in the lipid layer; (**C**) same as (**B**), top view. The area of a molecule projection onto the plane perpendicular to normal bilayer should be minimal.

The system tends to minimize the energy W. In the model, the minimum W can be achieved by two ways: (1) the molecule is pushed to the area of minimal lateral pressure; (2) the molecule turns so that the projection area A is the lowest. The last effects the molecule tilting inside the bilayer.

Lateral pressure profile is unique for a lipid composition, while projection area A depends on the molecule geometry. Since W depends on A linearly, for each lipid composition, the energy of the molecule is determined by its ability to turn within the bilayer so that area A is minimized.

Thus, the greater the change in the switch molecule projection area upon the *cis/trans* isomerization or open/closed reaction, the greater will be the produced lipid membrane distortion. Then, in search for an efficient optical switch for a lipid membrane, we should calculate the projection areas of the switch molecules in *cis* and *trans* (or open and closed) configurations and the difference between them.

2.3. Calculation Algorithm

Each of the molecules presented at Figure 1 in *cis*, *trans* or open and closed configurations was built in a chemical editor (we used Marvin Sketch, but any other will do). Then, geometries were optimized using quantum mechanics approaches in the ORCA [21] software package in two steps. First, the Hartree–Fock method utilizing the def2-SVP [22] basis was used. Next, the structure was optimized according to the B3LYP approach on the def2-TZVPP [22] basis. These yielded accurate geometries of the molecules (Figure 3A). The geometries are coordinates of atom centers. They were complemented with refined

van der Waals radii of the atoms [23] to build molecule surfaces; that is, define coordinates of points on the molecular surface (Figure 3B).

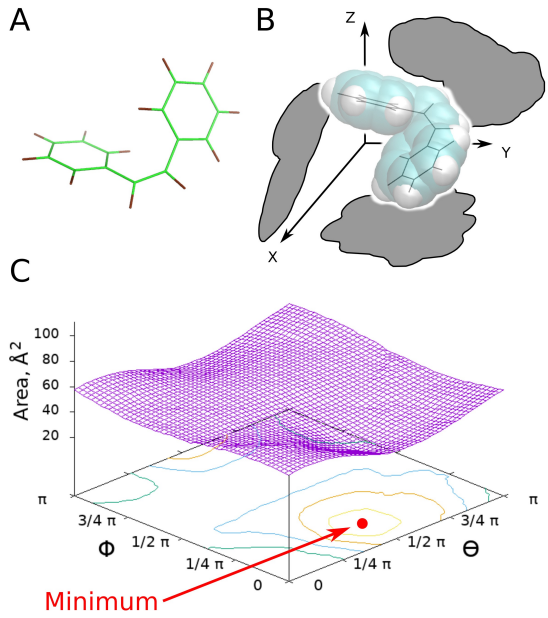

Figure 3. Algorithm of the projection area calculation. (**A**) Optimized geometry of *cis* stilbene. (**B**) *cis* stilbene with accurate van der Waals radii and its projections onto three planes. (**C**) Change in the *XY* projection area upon the molecule rotation around the *X* (angle Θ) and *Y* (angle Φ) axes.

The coordinate system was oriented in such a way that the *Z* axis was parallel to the normal bilayer. A plain *XY* was parallel to the bilayer surface. The molecule rotation around the *Z* axis did not lead to changes in the area of *XY* projection. The molecule was rotated independently around the *X* (angle Θ) and Y (angle Φ) axes with an increment of 0.0628 radian over 360 degrees (6.28 radian). For each pair of rotation angles, Θ and Φ, the projection area on the *XY* plain was calculated using the coordinates of the molecule surface (Figure 3C). Maximum and minimum projection areas were selected from the data set.

3. Results and Discussion

3.1. UV-Switch Geometry

Traditional 2D representation of molecules (Figure 1) does not always provide the correct idea of a molecule spatial structure. Optimized geometries of optical switches in *trans* and *cis* configurations are presented in Figure 4A. The geometrical parameters are reported in Table 1. For example, spatial configurations of a retinal analog NAIP and an overcrowded alkene OHBP are not planar. At the same time, stilbene, stiff-stilbene, azobenzene, GFP chromophore, and hemithioindigo are planar molecules. NABP is not planar, however, a deviation from plain in this case is much lower than for NAIP or OHBP. Figure 4B and Table 2 represent optimized geometries and parameters of O/C switches.

In a simplistic way, molecules can be viewed as rotational ellipsoids. There are two kinds of ellipsoids: prolates, which are elongated along the rotation axis, and oblates, which are flattened along the rotation axis.

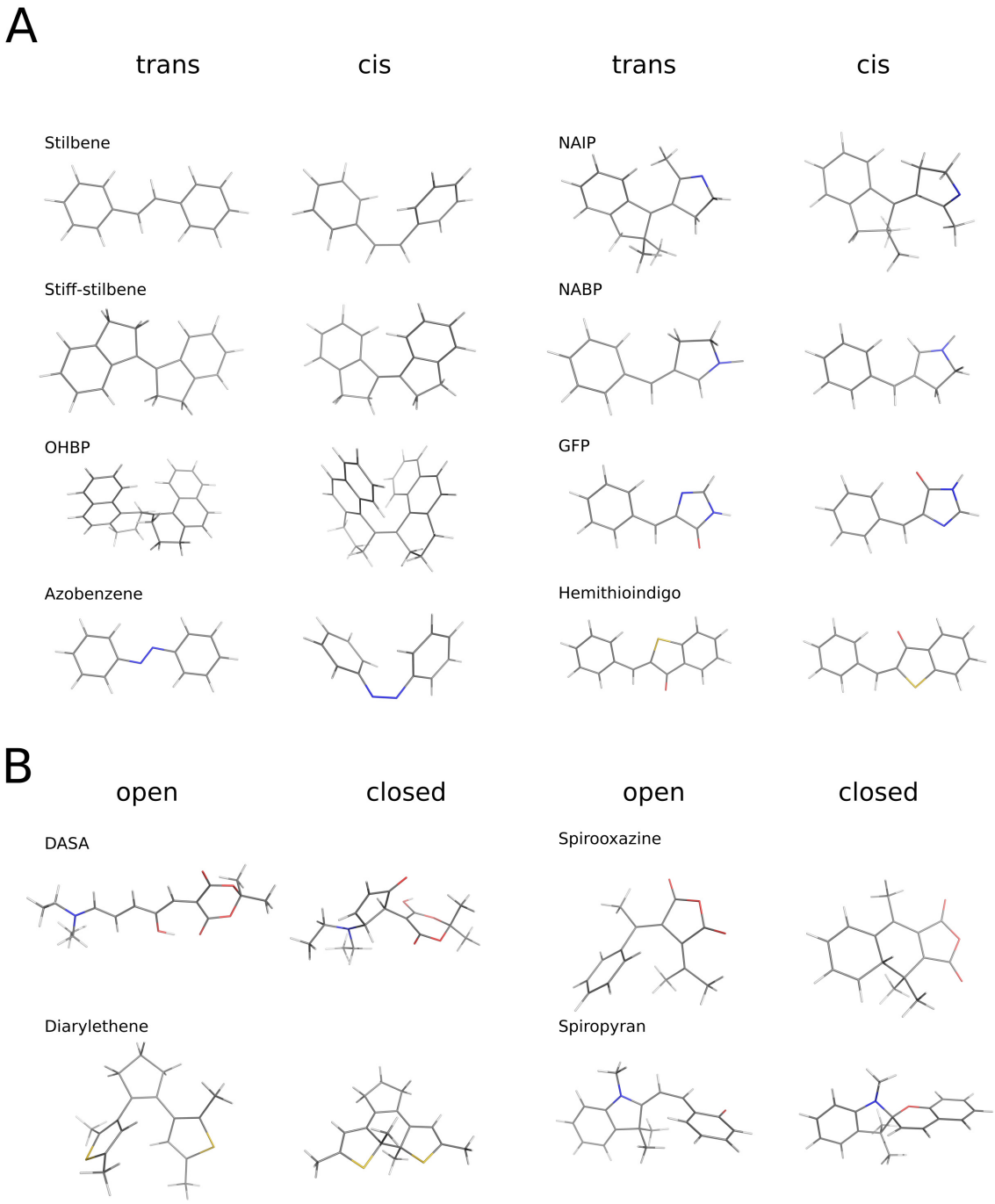

Figure 4. Optimized geometries of photoswitches in *trans*, *cis* (**A**), and open/closed (**B**) configurations.

Table 1. Characteristics of E/Z optical switches in *cis* and *trans* configurations.

Isomer	Parameter	Stilbene	Stiff-Stilbene	OHBP	Azobenzene	NAIP	NABP	GFP	Hemithioindigo
Trans	A_{max} (Å^2)	78.04	93.44	107.3	76.28	77.78	67.72	69.02	90.23
-	A_{min} (Å^2)	21.21	30.87	61.73	21.27	46.79	28.22	22.61	24.89
-	A_{max}/A_{min}	3.68	3.03	1.74	3.59	1.66	2.4	3.05	3.63
Cis	A_{max} (Å^2)	68.65	84.95	96.05	59.6	78.01	78.03	68.1	86.49
-	A_{min} (Å^2)	35.30	40.38	65.06	36.55	43.18	28.71	22.28	24.63
-	A_{max}/A_{min}	1.94	2.1	1.48	1.63	1.81	2.54	3.06	3.51

Table 2. Characteristics of O/C optical switches in open and closed configurations.

Isomer	Parameter	DASA	Diarylethene	Spirooxazine	Spiropyran
Open	A_{max} (Å^2)	97.22	82.29	74.53	85.90
-	A_{min} (Å^2)	39.10	62.18	46.65	46.75
-	A_{max}/A_{min}	2.49	1.32	1.60	1.84
Close	A_{max} (Å^2)	94.75	85.75	78.19	82.18
-	A_{min} (Å^2)	49.90	50.41	41.89	44.88
-	A_{max}/A_{min}	1.90	1.70	1.87	1.83

Trans isomers of stilbene, azobenzene, GFP chromophore, and hemithioindigo are elongated. The ratio between the maximum projection area to the minimum projection area of these molecules exceeds three (Table 1). These molecules can be referred to as prolates. Among O/C switches, only DASA in the open configuration could be referred to as a prolate.

The overcrowded alkene, NAIP, as well as spiopyran, spirooxazine and diarylethene are molecules with the least difference between the largest and the smallest projection areas These molecules are described as oblates.

The spaces of values of XY plain projection areas of each molecule are presented in Figure 5. For prolates (*trans*-stilbene, *trans*-azobenzene, GFP, hemithioindigo in both *cis* and *trans* configurations and DASA in open configuration) the range of the values is higher, with pronounced extremums. On the contrary, for oblates (*cis*-stilbene, *cis*-azobenzene, NABP, and OHBP in both *cis* and *trans* configurations, spiro-compounds and diarylethene in both open and closed configurations), the space is rather flat, and the extremums are not pronounced.

3.2. Trans/cis (Open/Closed) Transition, and Change in the Projection Area of the Molecules

Shape of the molecule changes upon transition from *trans* into *cis* (or from open into closed) configuration (Figure 4). Stilbene, stiff-stilbene, and azobenzene turn from planar into non-planar molecules. OHBP and NAIP remain non-planar; GFP chromophore and hemithioindigo, on the contrary, remain planar. NABP in both *cis* and *trans* configurations remains somewhat non-planar. Spiro-compounds and diarylethene are non-planar in any configuration.

A change in the configuration leads to a change in the projection area (Figure 5 and ΔA_{min} parameter (Tables 3 and 4)). The space of projection areas strongly changes for stilbene, azobenzene, and DASA, and remains practically unchanged for GFP chromophore, hemithioindigo, and NAIP. The space of projection areas of spiro-compounds and diarylethene changes but not so strongly as for stilbene and azobenzene.

The *trans/cis* transition causes prolate stilbene, azobenzene, and DASA to become oblate. Their spaces of values lose extremums and become flatter.

To evaluate the molecule potency as a membrane optical switch, a simple criterion can be used. Since we assume that a molecule takes on the orientation producing the smallest projection area A_{min}, the more A_{min} changes upon the transition from *trans* to *cis*, the more efficient is the optical switch. The change can be evaluated by the ratio

$$S = \frac{A_{min}^{cis}}{A_{min}^{trans}} \qquad or \qquad S = \frac{A_{min}^{close}}{A_{min}^{open}} \tag{2}$$

where A_{min}^{cis} and A_{min}^{trans} are the minimal projection areas for *cis* and *trans* conformers of a E/Z switch, respectively. and A_{min}^{close} and A_{min}^{open} are minimal projection areas for closed and open configurations of a O/C switch, respectively. The higher the S value is, the better.

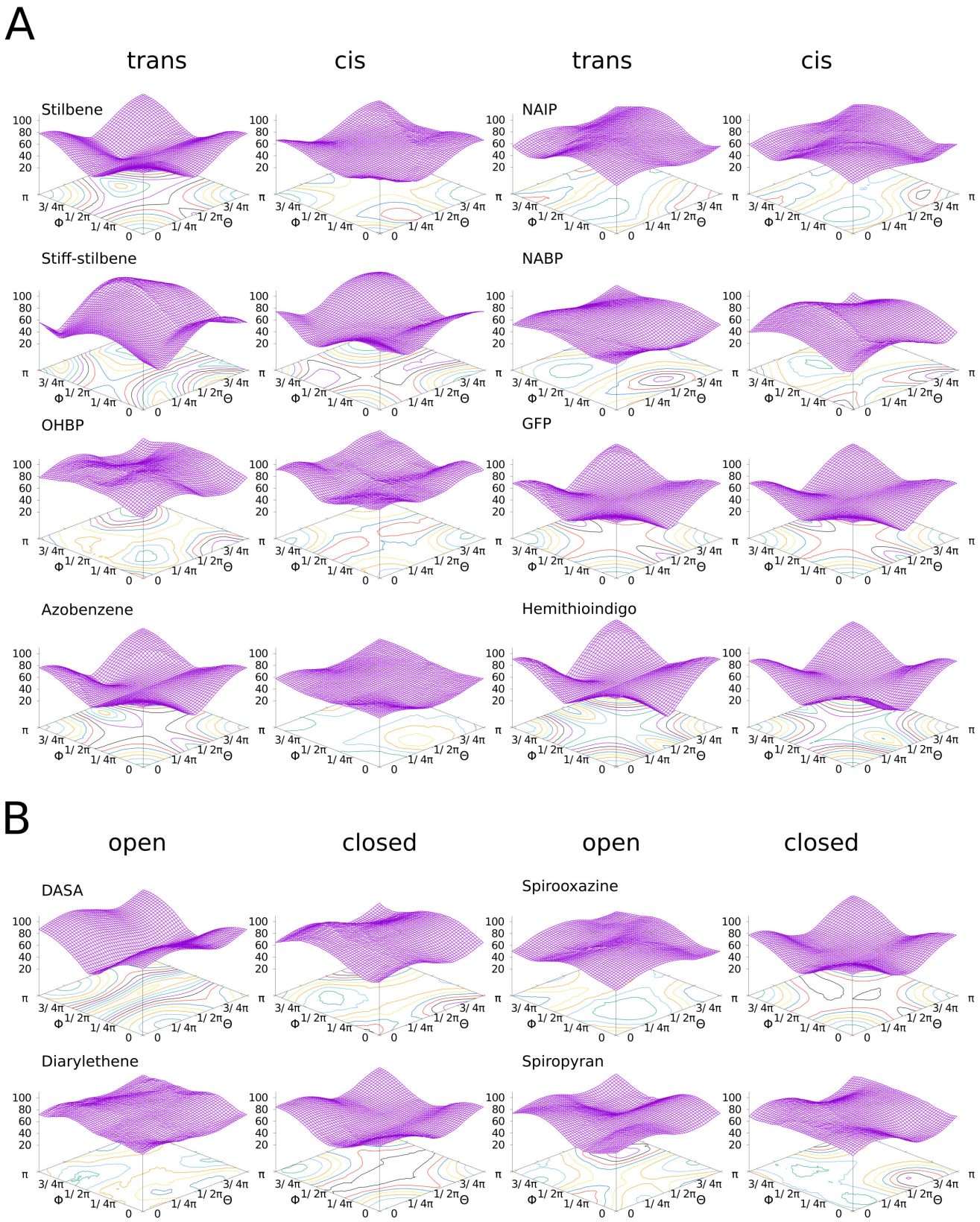

Figure 5. The space of the projection areas A (Å^2) of the molecules onto XY plane obtained upon scanning of the projection area upon rotation of the molecule over Θ and Φ. (**A**) E/Z-switches. (**B**) O/C-switches.

According to Tables 3 and 4, the most promising optical switches among those analyzed herein for lipid membranes are stilbene and azobenzene. For example, the minimum projection area of azobenzene upon the *trans/cis* transition increases by over 70% (as in the case of azobenzene). At the same time, the projection area of optical switches based on retinal analogs (NABP), GFP chromophore, and hemithioindigo practically does not change (below 2%). The latter are not suitable for application as optical switches in membranes. O/C-switches does not demonstrate high *S* values. These should not be as efficient as azobenzene and stilbene derivatives.

Table 3. Change of the geometry upon the *cis/trans* transition.

	Stilbene	**Stiff-Stilbene**	**OHBP**	**Azobenzene**	**NAIP**	**NABP**	**GFP**	**Hemithioindigo**
S	1.66	1.31	1.05	1.72	0.92	1.02	0.99	0.99
ΔA_{min} (Å^2)	12.09	9.51	3.33	15.28	3.61	0.49	5.94	0.26

Table 4. Change of the geometry upon the open/closed transition.

	DASA	**Diarylethene**	**Spirooxazine**	**Spiropyran**
S	1.28	0.81	0.90	0.96
ΔA_{min} (Å^2)	10.0	11.77	4.76	1.87

3.3. Structural Features of Promising Optical Switches

To find structural features of optical switches that make them promising for use in lipid membranes, we analyzed the geometry of the isomerizable double bond (Table 5). Values in columns corresponding to the compounds with the highest ratio *S* are highlighted in bold. (For atom numeration, see Figure 1).

Table 5. Geometry of the isomerizable double bond in optical switches.

Isomer	**Parameter**	**Stilbene**	**Stiff-Stilbene**	**OHBP**	**Azobenzene**	**NAIP**	**NABP**	**GFP**	**Hemithioindigo**
Trans	Dihedral angle° (1-2-3-4)	**180**	179.8	155	**180**	167.1	178.6	180.0	180.0
-	Angle° (1-2-3)	**127.1**	125.1	123.4	**116.6**	126.4	128.9	130.3	119.5
-	Angle° (2-3-4)	**127.1**	125.1	123.4	**116.6**	130.5	126.4	122.3	132.6
Cis	Dihedral angle° (1-2-3-4)	**4.5**	9.9	16.9	**5.4**	10.3	2.0	0.1	0
-	Angle° (1-2-3)	**129.7**	123.2	123.6	**124.4**	131.4	129.0	134.9	131.8
-	Angle° (1-2-3)	**129.7**	123.2	123.6	**124.4**	133.1	132.2	132.6	136.2

The highest *S* values are characteristic of molecules that are plain in the *trans* configuration (dihedral angel equals 180°) and have a dihedral angle other than 0° upon the transition to a *cis* configuration. In such molecules, substituent groups do not prevent the formation of a plain structure in the *trans* configuration and, on the contrary, hinder plain configuration for the *cis* isomer. Then, elongated molecules with substituents in *meta* and *para* positions with respect to the isomerizable double bond should be promising optical switches. To verify the hypothesis, we studied molecules with methyl, cyclopentyl, and cyclohexyl substituents (Figure 6) in either one of the molecule fragments or both. All molecules in Figure 6 can be described as prolates, with one dimension exceeding the other two. The ratio of maximum and minimum projection areas is over 3 for all of them (Table 6). All these molecules turned out to have a high *S* value and thus can be used as optical switches in lipid membranes.

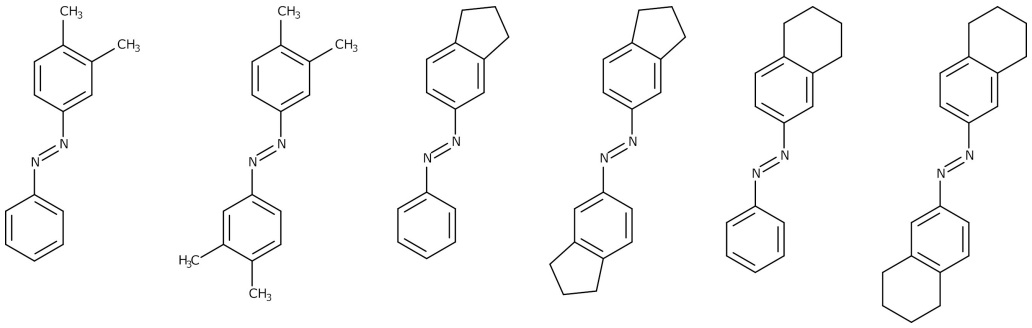

Figure 6. Predicted structures of efficient optical switches for lipid membranes.

Table 6. Characteristics of predicted optical switches (depicted in Figure 6) in *cis* and *trans* configurations.

Isomer	Parameter	Dimethyl mono	Dimethyl bis	Cyclopentyl mono	Cyclopentyl bis	Cyclohexyl mono	Cyclohexyl bis
Trans	A_{max} (Å^2)	85.71	99.56	87.03	98.65	92.66	108.41
-	A_{min} (Å^2)	26.83	28.92	28.32	32.73	30.20	33.73
-	A_{max}/A_{min}	3.19	3.44	3.07	3.01	3.07	3.21
Cis	A_{max} (Å^2)	70.27	79.44	73.09	80.94	78.22	93.04
-	A_{min} (Å^2)	42.47	50.1	42.24	52.71	44.12	51.21
-	A_{max}/A_{min}	1.65	1.59	1.73	1.54	1.77	1.82
-	S	1.58	1.73	1.49	1.61	1.46	1.52
-	ΔA_{min} (Å^2)	15.44	21.18	13.92	19.98	13.92	17.48

4. Conclusions

Among optical switches used today, those based on stilbene and azobenzene are the most suitable for lipid membranes. They are characterized by the highest change of the area of projection onto the bilayer. The design of new optical switches for lipid membranes should take into account that substituents at the double bond that decrease the angle of the *sp2* atom, for example the 5-membered cycle, decreases the *S* factor: the *cis* isomer is as planar as the *trans* isomer. At the same time, spatial hinderances leading to non-planar *trans* isomers decrease the *S* factor as well. Efficient optical switches are planar elongated molecules, in which atoms of isomerizable double bond have no additional substituents, while substituents of the fragments adjacent to the double bond prevent formation of the planar molecule in the *cis* configuration to make the *S* factor high.

Funding: This research was funded by the RFBR grant No. 20-03-00770 A.

Institutional Review Board Statement: Not appliable.

Informed Consent Statement: Not appliable.

Data Availability Statement: Not appliable.

Conflicts of Interest: The author declares no conflict of interest.

References

1. Fujiwara, H.; Yonezawa, Y. Photoelectric response of a black lipid membrane containing an amphiphilic azobenzene derivative. *Nature* **1991**, *351*, 724–726. [CrossRef]
2. Song, X.; Perlstein, J.; Whitten, D. Supramolecular aggregates of azobenzene phospholipids and related compounds in bilayer assemblies and other microheterogeneous media: Structure, properties, and photoreactivity. *J. Am. Chem. Soc.* **1997**, *119*, 9144–9159. [CrossRef]
3. Hamada, T.; Sugimoto, R.; Nagasaki, T.; Takagi, M. Photochemical control of membrane raft organization. *Soft Matter* **2011**, *7*, 220–224. [CrossRef]
4. Frank, J.; Franquelim, H.; Schwille, P.; Trauner, D. Optical Control of Lipid Rafts with Photoswitchable Ceramides. *J. Am. Chem. Soc.* **2016**, *138*, 12981–12986. [CrossRef]

5. Saitov, A.; Akimov, S.; Galimzyanov, T.; Glasnov, T.; Pohl, P. Ordered Lipid Domains Assemble via Concerted Recruitment of Constituents from Both Membrane Leaflets. *Phys. Rev. Lett.* **2020**, *124*, 108102. [CrossRef]
6. Frank, J.; Yushchenko, D.; Hodson, D.; Lipstein, N.; Nagpal, J.; Rutter, G.; Rhee, J.; Gottschalk, A.; Brose, N.; Schultz, C.; et al. Photoswitchable diacylglycerols enable optical control of protein kinase C. *Nat. Chem. Biol.* **2016**, *12*, 755–762. [CrossRef]
7. Frank, J.; Moroni, M.; Moshourab, R.; Sumser, M.; Lewin G.; Trauner, D. Photoswitchable fatty acids enable optical control of TRPV1. *Nat. Commun.* **2015**, *6*, 7118. [CrossRef]
8. Pfeffermann, J.; Eicher, B.; Boytsov, D.; Hannesschlaeger, C.; Galimzyanov, T.; Glasnov, T.; Pabst, G.; Akimov, S.; Pohl P. Photoswitching of model ion channels in lipid bilayers. *J. Photochem. Photobiol. B* **2021**, *224*, 112320. [CrossRef]
9. Georgiev, V.; Grafmüller, A.; Bléger, D.; Hecht, S.; Kunstmann, S.; Barbirz, S.; Lipowsky, R.; Dimova, R. Area Increase and Budding in Giant Vesicles Triggered by Light: Behind the Scene. *Adv. Sci.* **2018**, *5*, 1800432. [CrossRef]
10. García-Iriepa, C.; Marazzi, M.; Frutos, L.M.; Sampedro, D. E/Z Photochemical switches: Syntheses, properties and applications. *RSC Adv.* **2013**, *3*, 6241–6266. [CrossRef]
11. Lerch, M.M.; Szymanski, W.; Feringa, B.L. The (photo)chemistry of Stenhouse photoswitches: Guiding principles and system design. *Chem. Soc. Rev.* **2018**, *47*, 1910. [CrossRef] [PubMed]
12. Irie, M.; Fukaminato, T.; Matsuda, K.; Kobatake, S. Photochromism of diarylethene molecules and crystals: Memories, switches, and actuators. *Chem. Rev.* **2014**, *114*, 12174–12277. [CrossRef] [PubMed]
13. Li, Z.; He, C.; Li, P.; Zhu, Y.-P. Recent progress in all-visible-light-triggered diarylethenes. *Dye. Pigment.* **2020**, *182*, 108623. [CrossRef]
14. Bercovic, G.; Krongauz, V.; Weiss, V. Spiropyrans and spirooxazines for memories and switches. *Chem. Rev.* **2000**, *100*, 1741–1754. [CrossRef]
15. Leith, G.A.; Martin, C.R.; Mathur, A.; Kittikhunnatham, P.; Park, K.C.; Shustova, N.R. Dynamically controlled electronic behavior of stimuli-responsive materials: Exploring dimensionality and connectivity. *Adv. Energy Mater.* **2022**, *12*, 2100441. [CrossRef]
16. Ollila, O.H.S.; Risselada, H.J.; Louhivuori, M.; Lindahl, E.; Vattulainen, I.; Marrink, S.J. 3D Pressure field in lipid membranes and membrane-protein complexes. *Phys. Rev. Lett.* **2009**, *102*, 10–11. [CrossRef]
17. Mukhin, S.I.; Kheyfets, B.B. Analytical approach to thermodynamics of bolalipid membranes. *Phys. Rev. E* **2010**, *82*, 51901. [CrossRef]
18. Drozdova, A.A.; Mukhin, S.I. Lateral pressure profile in lipid membranes with curvature: Analytical calculation. *J. Exp. Theor. Phys.* **2017**, *125*, 357–363. [CrossRef]
19. Tretiakova, D.S.; Alekseeva, A.S.; Galimzyanov, T.R.; Boldyrev, A.M.; Chernyadyev, A.Y.; Ermakov, Y.A.; Batishchev, O.V.; Vodovozova, E.L.; Boldyrev, I.A. Lateral stress profile and fluorescent lipid probes. FRET pair of probes that introduces minimal distortions into lipid packing. *Biochim. Biophys. Acta (BBA)-Biomembr.* **2018**, *1860*, 2337–2347. [CrossRef]
20. Shchegravina, E.S.; Tretiakova, D.S.; Alekseeva, A.S.; Galimzyanov, T.R.; Utkin, Y.N.; Ermakov, Y.N.; Svirshchevskaya, E.V.; Negrebetsky, V.V.; Karpechenko, N.; Chernikov, V.P.; et al. Phospholipidic Colchicinoids as Promising Prodrugs Incorporated into Enzyme-Responsive Liposomes: Chemical, Biophysical, and Enzymological Aspects. *Bioconjug. Chem.* **2019**, *30*, 1098–1113. [CrossRef]
21. Neese, F. The ORCA program system. *WIREs Comput. Mol. Sci.* **2012**, *2*, 73–78. [CrossRef]
22. Weigend, F.; Ahlrichs, R. Balanced basis sets of split valence, triple zeta valence and quadruple zeta valence quality for H to Rn: Design and assessment of accuracy. *Phys. Chem. Chem. Phys.* **2005**, *7*, 3297–3305. [CrossRef] [PubMed]
23. Alvarez, S. A cartography of the van der Waals territories. *Dalt. Trans.* **2013**, *42*, 8617–8636. [CrossRef] [PubMed]